Video Article

Sequential *In vivo* Imaging of Osteogenic Stem/Progenitor Cells During Fracture Repair

Dongsu Park[1], Joel A. Spencer[2], Charles P. Lin[2], David T. Scadden[1]

[1]Center for Regenerative Medicine, Massachusetts General Hospital, Harvard Stem Cell Institute

[2]Wellman Center for Photomedicine and Center for Systems Biology, Massachusetts General Hospital, Harvard Medical School

Correspondence to: Dongsu Park at dongsu.park@bcm.edu, David T. Scadden at david_scadden@harvard.edu

URL: http://www.jove.com/video/51289
DOI: doi:10.3791/51289

Keywords: Medicine, Issue 87, Osteogenic Stem Cells, *In vivo* Imaging, Lineage tracking, Bone regeneration, Fracture repair, Mx1.

Date Published: 5/23/2014

Citation: Park, D., Spencer, J.A., Lin, C.P., Scadden, D.T. Sequential *In vivo* Imaging of Osteogenic Stem/Progenitor Cells During Fracture Repair. *J. Vis. Exp.* (87), e51289, doi:10.3791/51289 (2014).

Abstract

Bone turns over continuously and is highly regenerative following injury. Osteogenic stem/progenitor cells have long been hypothesized to exist, but *in vivo* demonstration of such cells has only recently been attained. Here, *in vivo* imaging techniques to investigate the role of endogenous osteogenic stem/progenitor cells (OSPCs) and their progeny in bone repair are provided. Using osteo-lineage cell tracing models and intravital imaging of induced microfractures in calvarial bone, OSPCs can be directly observed during the first few days after injury, in which critical events in the early repair process occur. Injury sites can be sequentially imaged revealing that OSPCs relocate to the injury, increase in number and differentiate into bone forming osteoblasts. These methods offer a means of investigating the role of stem cell-intrinsic and extrinsic molecular regulators for bone regeneration and repair.

Video Link

The video component of this article can be found at http://www.jove.com/video/51289/

Introduction

Degenerative bone diseases and age-related bone loss leading to a high risk of osteoporotic fracture has become a major challenge in public health[1]. Bone maintenance is controlled by bone-forming osteoblasts and bone-resorbing osteoclasts. Defects of bone forming cells are a main cause of age-related bone loss and degenerative bone diseases[2,3]. While extensive research has focused on the improvement of fracture healing, the discovery of reliable drugs to cure degenerative bone diseases and to reverse the weakness of osteoporotic fractures remains an important issue. Thus, studying the source of bone forming cells and their control mechanisms in bone regeneration and repair provides a novel insight to enhance skeletal regeneration and reverse bone loss diseases.

The existence of multipotent mesenchymal cells in bone marrow has been proposed based on the identification of clonogenic populations that could differentiate into osteogenic, adipogenic and chondrogenic lineages *ex vivo*[4]. Recently, multiple studies have reported that skeletal/mesenchymal stem cells (SSCs/MSCs) are a natural source of osteoblasts and are critical for bone turnover, remodeling, and fracture repair[5,6]. In addition, our lineage-tracing study revealed that mature osteoblasts have a unexpectedly short half-life (~60 days) and are continuously replenished by their stem/progenitor cells in both normal homeostatic and fracture repair conditions[6]. However, the *in vivo* identity of stem cells and how such cells react to fracture injury and supply bone-forming cells are unclear. Therefore, it is important to develop a method that is able to analyze the migration, proliferation and differentiation of endogenous SSCs/MSCs in under physiological circumstances.

Fracture repair is a multi-cellular and dynamic process regulated by an array of complex cytokines and growth factors[7]. The most popular approach for fracture studies is to use an animal model with long-bone fracture and to analyze bones by bone sectioning and immunofluorescent techniques[8-10]. This repair process can be monitored by multiple imaging techniques including micro-CT[11], near-infrared fluorescence[12], and chemiluminescence imaging[13]. However, each technique has certain limitations and there has been no effective way to monitor SSCs/MSC function at the cellular level *in vivo*. Recently, confocal/two-photon intravital microscopy has been developed and used to detect transplanted cancer cells and hematopoietic stem cells in the context of their bone marrow microenvironment even at single-cell resolution in living animals[14]. By combining this technology with a series of lineage tracing models, we were able to define that osteogenic stem/progenitor cells can be genetically marked by transient activation of the *myxovirus resistance*-1 (*Mx1*) promoter and *Mx1*-induced progenitors can maintain the majority of mature osteoblasts over time but do not participate in the generation of chondrocytes in the adult mouse[6]. In addition, we demonstrated that *Mx1*-labeled OSPCs supply the majority of new osteoblasts in fracture healing[6].

Here, using osteo-lineage tracking models and intravital microscopy, a protocol is provided to define the *in vivo* kinetics of $Mx1^+$ osteogenic stem/progenitor cells in fracture repair. This protocol offers sequential imaging to track the relocation of osteogenic stem/progenitors into fracture sites and the quantitative measurement of osteoprogenitor expansion in the early repair process. This approach may be useful in multiple contexts including the evaluation of therapeutic candidates to improve bone repair.

Copyright © 2014 Journal of Visualized Experiments

Protocol

1. Mice and Preconditioning

Note: All mice were maintained in pathogen-free conditions and all protocols were approved by the Institutional Animal Care and Use Committee (IACUC) at the Massachusetts General Hospital. All surgery should be performed under sterile condition using autoclaved sterile equipment. *Mx1-Cre*[15], *Rosa26-loxP-stop-loxP-EYFP* (Rosa-YFP), and *Rosa26-loxP-stop-loxP-tdTomato* (Rosa-Tomato), were purchased from Jackson Laboratories. *Osteocalcin-GFP* mice were provided by Dr. Henry Kronenberg. For the quantitative analysis of OSPC migration and proliferation *in vivo*, *Mx1-Cre*$^{+}$*Rosa-YFP*$^{+}$ (single color-reporter) mice were used. For more detailed tracking of their differentiation into *Osteocalcin*$^{+}$ mature osteoblasts, we used trigenic *Mx1-Cre*$^{+}$*Rosa-Tomato*$^{+}$*Ocn-GFP*$^{+}$ mice.

1. To label *Mx1*$^{+}$ cells *in vivo*, prepare polyinosinic-polycytidylic acid (pIpC, 2.5 mg/ml) in sterile PBS solution and inject 200 µl for 20 g of *Mx1-Cre*$^{+}$ reporter mouse intraperitoneally once every other day for 10 days.
2. To eliminate resident *Mx1*$^{+}$ hematopoietic cells, irradiate mice with a single dose of 9.5 Gy. After 24 hr of irradiation, transplant wild type bone marrow cells (1x10^{6} cells/mouse) intravenously[16]. Note: Since *Mx1*-inducible cells include hematopoietic cells and hematopoietic-derived osteoclasts, the elimination of *Mx1*$^{+}$ hematopoietic cells improves the imaging quality and quantitation of *Mx1*$^{+}$ osteogenic cells.
3. After bone marrow transplantation, monitor animals for four to six weeks in order to achieve a successful repopulation of donor marrow cells.

2. Mouse Preparation

1. Anesthetize mouse by intraperitoneal injection of 50 µl of ketamine/xylazine (100 mg/kg, xylazine 12 mg/kg body weight) using an IACUC-approved procedure. Note: Duration of the effect may be extended by an additional dose of ketamine/xylazine.
2. Determine if the mouse is fully anesthetized by the lack of response to toe and/or tail pinches. (Optional) When the mouse is anesthetized, secure an isoflurane gas mask over the nose by taping. Adjust the level of isoflurane to ensure the animal is fully sedated.
3. Clip the scalp hair using an electric trimmer or small scissors. Remove the hair fragments and sterilize the exposed skin with 70% alcohol swab. Apply tear gel to prevent corneal dehydration.

3. Microfracture Injury

1. After ensuring the animal is fully sedated, make a single reverse L-shaped incision to open the scalp skin. Briefly, make a first transverse incision (less than 1 cm) starting from one ear to another ear. Turn ~60° and continue to incise toward the nose until ~2-3 mm away from nose. Note: This incision minimizes the formation of scar tissues above the area to be imaged.
2. Separate the skin flaps by pulling toward the sides with forceps. Both frontal bones and the intersection of sagittal and coronal sutures should be clearly exposed.
3. Clean the open surface by flushing with sterile PBS and gentle wiping with sterile gauze or cotton swabs until all the residual hairs are eliminated.
4. To generate microfractures on the calvarium, hold the mouse head with one hand and a 30 G needle with another hand. Make a micro-puncture (~0.2 mm diameter wound with < 1 mm depth) on the left frontal bone near the intersection of the sagittal and coronal sutures by inserting the tip of a 30 G needle with gentle pressure and twisting motion. Caution: It is critical to avoid the needle from penetrating into the brain, thereby minimizing bleeding and tissue damage.
5. Switch to a bigger needle (20 or 25 G) and widen the puncture hole by twisting the needle (~0.5 mm diameter).
6. Repeat step 3.3-3.5 to generate second puncture on the contralateral frontal bone.
7. Wipe out the injured spots by continuous dropping of PBS until the bleeding stops.
   Note: Bleeding on fracture sites will interfere with appropriate imaging and induce scar formation.
8. Apply a drop of sterile physiological saline solution or 2% Methocel on the skull to avoid drying. Note: Do not allow the skull surface to dry, which will reduce image clarity. It is important to use a sufficient amount of gel or saline to cover the area.

4. Intravital Imaging

1. (Optional) Before imaging, some mice are injected with a vascular dye to visualize the blood vessels. Inject retro-orbitally with 20 µl of non-targeted Qtracker 705 (2 µM solution in 50 mM borate buffer) diluted in 80 ml of PBS. Use an insulin syringe to minimize reagent waste. If the signal is not sufficiently bright, additional amounts might be required.
2. Turn on the scanner. Note: A polygon-based laser scanner allows simultaneous multi-channel image acquisition at video rate (30 frames per sec). Video rate scanning is very important for live animal imaging.
3. Turn on the multi-photon laser (femto-second titanium:sapphire laser). Set the wavelength to 880 nm and adjust the power for second harmonic generation imaging (440 nm) of the bone. For GFP and tdTomato excitation, turn on the 491 nm and 561 nm solid-state lasers.
4. Turn on the PMT (photomultiplier tube) detectors for each signal (a 435 ± 20 nm band-pass filter for second harmonic generation, a 528 ± 19 nm band-pass filter for GFP, and 590 ± 20 for tdTomato.) (Optional) Use a 638 nm helium–neon laser and a PMT with a 695 ± 27.5 nm band-pass filter to detect Qtracker 705 signal.
5. Place the animal on a XYZ-axis motorized microscope stage. Keep the mouse in the most comfortable position with an electric heating pad to help maintain body temperature (this reduces the risk of animal loss). Use tape to hold the mouse to minimize movement during imaging and to keep the imaged area as horizontal as possible.
6. Apply a drop of warm 2% methylcellulose gel or physiological saline solution on the skull to avoid drying. Put a cover glass on the imaging area. Use a low magnification lens (30x water-immersion objective with 0.9 NA) to scan the calvaria.

Copyright © 2014 Journal of Visualized Experiments

7. Using the XYZ-axis controller, find the surface of calvaria by detecting the SHG signal from bones and identify a crucial landmark location, such as the intersection between the sagittal sutures and coronal sutures. Acquire an image and record the XYZ coordinates.
8. Continue to search for the location of the injury by observing SHG and fluorescence signals.
9. When injury sites or the region of interest are found, acquire an image of the best focal plane containing SHG and fluorescence signals from the cells of interest. Save XYZ coordinates and the distance to the intersection of the sagittal and coronal sutures to define their precise location for the next rounds of imaging.
10. To collect 3D cellular and bone structures of fracture injury, record images by Z-stacks (2 - 5 µm interval) with ~100 µm depth from endosteal bone surface. After the completion of imaging of one side of injury, repeat imaging process for next injury sites.

5. Post Operation Procedures

1. After imaging, rinse imaging site with sterile saline solution to remove the methylcellulose gel from the skull. Using a sterile cotton swab, apply a small amount of triple antibiotic ointment on the surface. Cover the skin flaps and re-close the scalp by surgical suturing. This can be done with a hypoallergenic suturing thread (absorbable polyglactin suture) and 5-0 size suture needle. Caution: Good suturing technique minimizes scar formation.
2. Treat all animals with IP injection of 0.05-0.1 mg/kg buprenorphine every 12 hr for 48 hr following surgery. Keep animals in a warm recovery chamber until they regain sufficient consciousness. After 3 to 5 days, reopen the suture and repeat intravital imaging steps to track the cellular change during fracture healing.

Representative Results

The stabilized long bone fracture model has been popular in fracture studies. However, long bone or large fracture models cause multiple tissue damage and therefore, have a limitation in quantitative measurement of bone cell function. We developed a minimally invasive injury (less than 1 mm diameter with minimal or no invasion into the dura mater) on calvarial frontal bones with needle drilling (**Figures 1A-1C**). We chose a top view of the calvarial frontal bones for *in vivo* live imaging of microfractures because this bone has a flat and thin bone structure with bone marrow, permitting clear imaging of injured bone, bone cells, and vasculature without the interference of other tissues (**Figure 1C**). We observed that this microfracture recapitulates many characteristics of large fracture injuries including soft callus formation followed by mineral deposition and new bone formation (data not shown).

Sequential *in vivo* imaging of *Mx1*$^+$ osteogenic stem progenitor cells. We next tested if this method is capable of tracking a particular osteogenic cell population during fracture healing. Previously, we developed the trigenic Mx1/Tomato/Ocn-GFP dual reporter mice by crossing *Mx1-Cre* mice with *Rosa26-Tomato* reporter and *osteocalcin-GFP* mice (**Figure 2A**)[6]. The advantage of this model is the differential labeling of osteogenic stem/progenitors and mature osteoblasts. By pIpC administration, the *Mx1*$^+$ OSPCs are specifically labeled by the tomato expression, whereas mature osteoblasts differentiated from *Mx1*-induced OSPCs express Tomato and GFP. However, pre-existing osteoblasts and mature osteoblasts from *Mx1* non-inducible progenitors express GFP alone (**Figure 2B**). After irradiation and bone marrow replacement, we generated two microfractures on the frontal bones of these mice. We confirmed that the area of each fracture was detected by a single field of view with our 30x objective. Sequential 3D-intravital imaging of microfractures showed the relocation of Tomato$^+$ OSPCs in the site of the fracture at day 2 and their expansion at day 5. There were no or undetectable GFP$^+$ osteoblasts at this time. On day 12, a subset of osteoprogenitors near the fracture surface initiated the differentiation of osteoblasts (Tomato$^+$GFP$^+$). Subsequently, the accumulation of new osteoblasts and new bone formation (analyzed by second harmonic generation, blue) were obvious on day 21, indicating that the migration and proliferation of osteogenic progenitor cells is a major mechanism to supply new osteoblasts participating in fracture healing (**Figure 2C**).

Kinetics of osteogenic stem/progenitors in fracture repairs. To test whether our method provides a consistent and quantitative output of osteoprogenitor numbers during fracture healing, we used the Mx1/YFP mouse as a simple lineage-tracking model and tracked *Mx1*$^+$ OSPCs in early fracture repair. After *Mx1*$^+$ marrow cells were replaced by wild type marrow, we generated six independent microfractures (two/mouse) on Mx1/YFP mouse calvaria. When Mx1/YFP$^+$ OSPCs were tracked for 14 days after injury, we consistently observed that small numbers of progenitors were detected at the injury site by 3 days. The numbers continuously increased at day 7, reaching peak population at day 10 and sustaining by 14 days (**Figure 3A**). We quantified the kinetics of osteoprogenitor numbers by measuring YFP signal intensity (image processing and analysis with the ImageJ program). We repeated this experiment with a similar output, suggesting the consistency of our approach (**Figure 3B**).

Copyright © 2014 Journal of Visualized Experiments

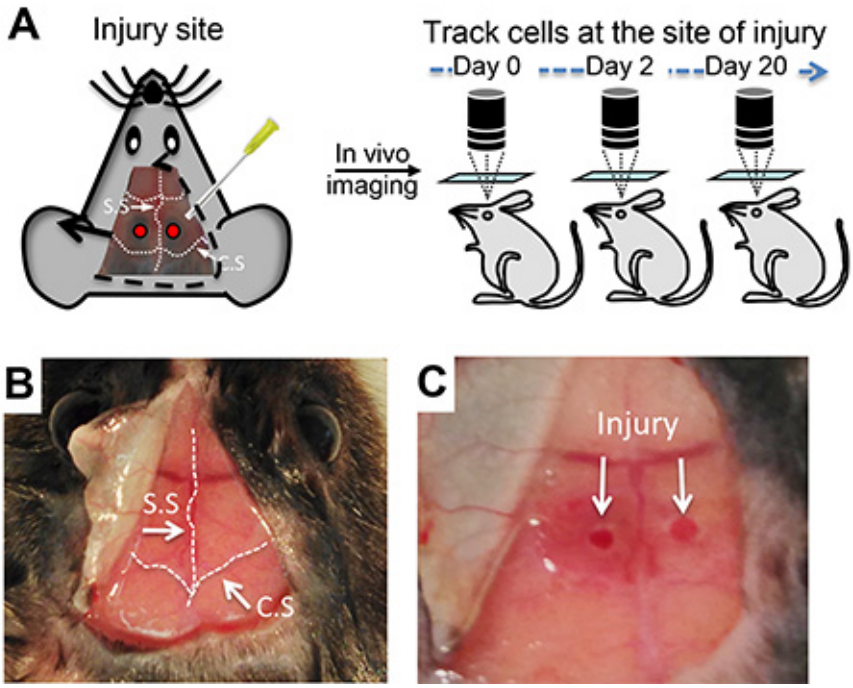

Figure 1. ***In vivo*** **imaging of mouse calvarial injury. (A)** Schematic representation of microfractures on the mouse frontal bones near the intersection of the coronal (C.S) and sagittal sutures (S.S) and sequential intravital imaging. **(B)** Surgical exposure of mouse calvaria before injury. **(C)** Representative microfracture injuries on mouse calvaria for intravital imaging. Please click here to view a larger version of this figure.

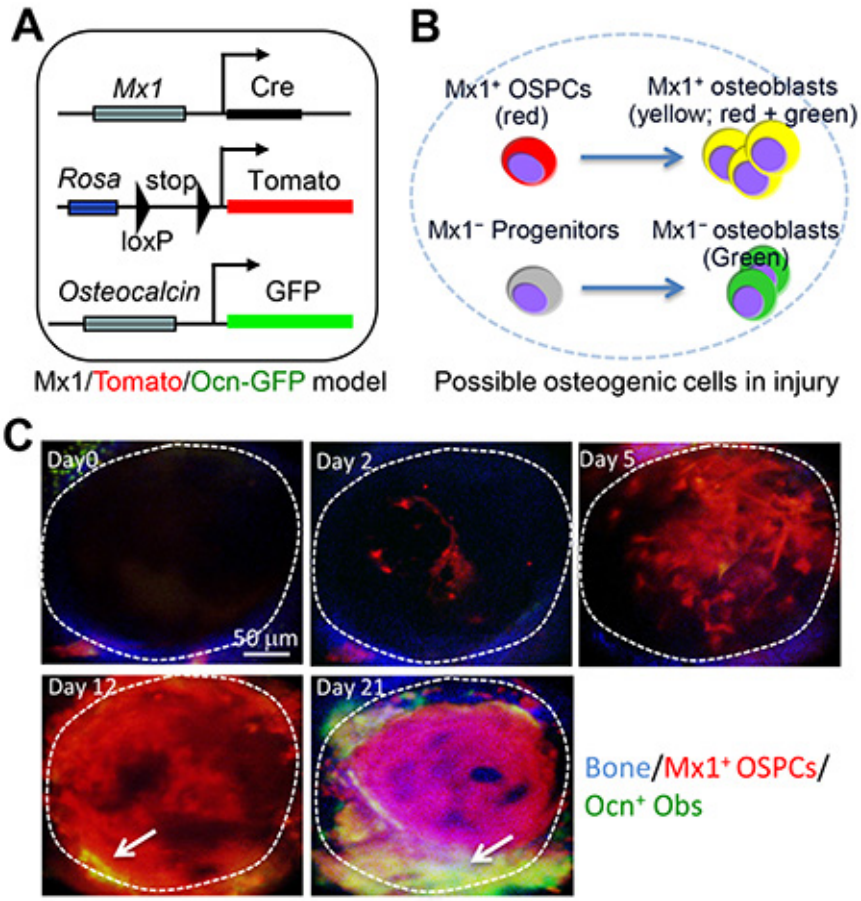

Figure 2. *In vivo* tracking of OSPCs at the injury sites. (A) Schematic representation of trigenic Mx1/Tomato/Ocn-GFP mouse. **(B)** This diagram illustrates possible fluorescent cell populations that appear at injury sites of trigenic Mx1/Tomato/Ocn-GFP mouse. Red represents *Mx1*$^{+}$ OSPCs expressing Tomato. Yellow represents mature osteoblasts (Tomato^{+}GFP^{+}) differentiated from *Mx1*$^{+}$ OSPCs whereas green represents new osteoblasts from pre-existing osteoblasts (GFP^{+}) or *Mx1* non-inducible (*Mx1*$^{-}$) progenitors. **(C)** Sequential intravital imaging of *Mx1*$^{+}$ OSPCs and osteoblasts at the injury sites. Tomato^{+} osteoprogenitors and GFP^{+} osteoblasts near the injury on Mx1/Tomato/Ocn-GFP mouse calvaria were imaged immediately after injury (day 0) and at the indicated times after injury. Arrows indicate osteoblasts derived from *Mx1*$^{+}$ OSPCs (yellow). Blue, bone. The dotted circle represents the entire (single) fracture site. Please click here to view a larger version of this figure.

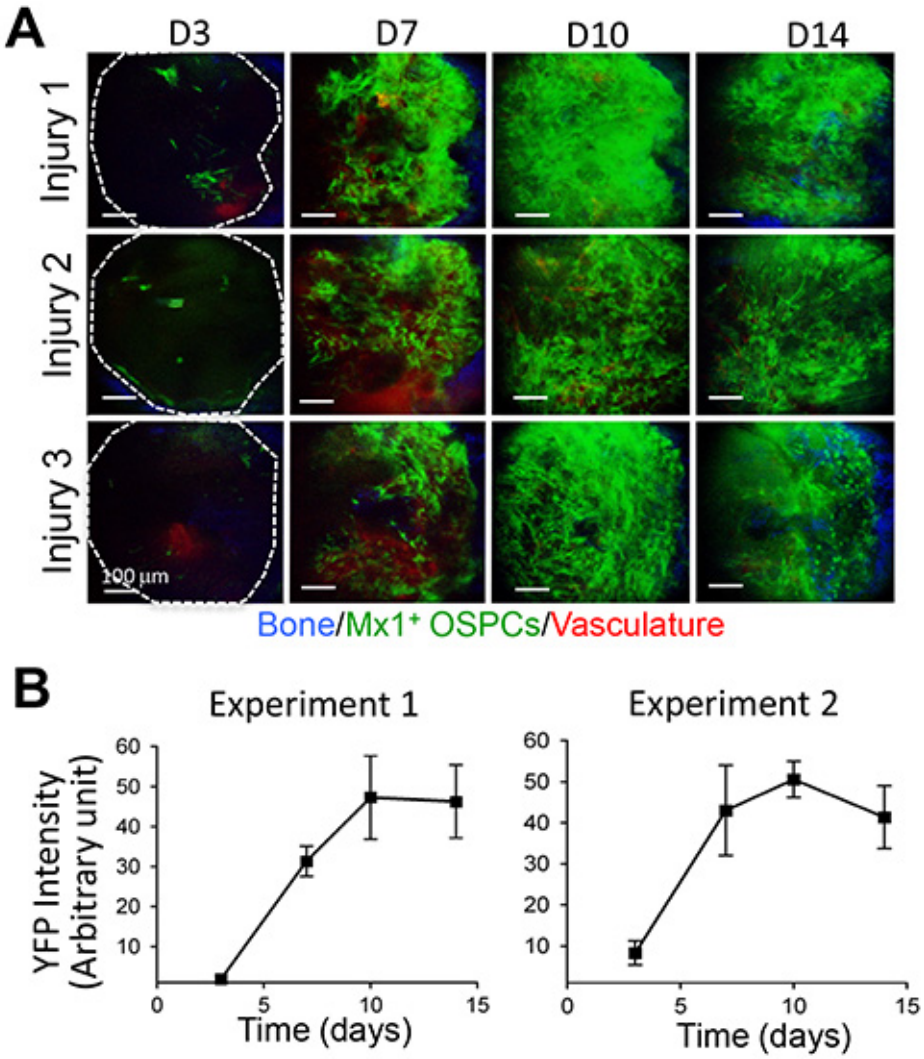

Figure 3. Consistent and quantitative measurement of *Mx1*-induced OSPCs during fracture healing. (A) Three independent injuries on Mx1/YFP mouse calvaria were sequentially imaged immediately after injury (day 0) and at the indicated times after injury. **(B)** Quantitative measurement of *Mx1*$^+$ osteogenic stem/progenitor cells. The kinetics of *Mx1*+ OSPC expansion at injury sites was measured by YFP signal intensity using ImageJ. Graphs show two independent experiments with the average of six injuries in each experiment. Blue, bone; green, *Mx1*$^+$ osteogenic stem/progenitor cells; red, vasculature (Q-dots). Scale bars are 100 µm (A). Please click here to view a larger version of this figure.

Discussion

The regulation of skeletal stem cells may be of great importance for defining better methods to achieve bone regeneration. Quantitative and sequential imaging at the cellular level has been technically challenging. Although the mouse long-bone fracture model has been widely used and suitable for biomechanical studies [17], its deep tissue location, uneven fracture size, soft tissue damage, and the application of stabilizing fixators have limited sequential intravital imaging. Here, a method to overcome these limitations by the combination of confocal/two-photon intravital microscopy and a mouse calvarial fracture model is provided. This approach with osteogenic stem/progenitor lineage tracking demonstrates its capability for real-time, *in vivo* imaging of osteogenic stem/progenitors in fracture repair.

A major technical challenge in this method is to obtain consistent and high quality images over time. High quality images with maximum imaging depth depend on the brightness of the fluorescent reporters and the tissue condition of the imaging area. In addition, minimizing laser exposure to avoid tissue damage and photobleaching is important for long-term sequential imaging. Rapid scanning using the video rate platform is helpful for this purpose. If a single field of view cannot cover whole injury, the area can be mapped by taking montage images to cover most of the fracture sites. It is important to compromise between the quality of the Z-stack and the amount of information acquired during the whole imaging session. For example, Z-stacks with many slices (*e.g.* 1-2 µm steps) and high definition are easier to analyze further; however, they require long-term laser exposure leading to a higher degree of laser-induced photobleaching.

Since sequential *in vivo* imaging of fracture injury necessitates the repetitive surgical opening of skin and bone surface, fibrotic scar formation on the surface of calvaria is a common problem that interrupts deep tissue imaging and yields high background florescence. Skilled suture

techniques and minimum bleeding is critical to reduce scar formation. In general, three to five time repeat imaging can be achieved without significant loss of image quality.

Given the possibility of repeat imaging, the easy and accurate control of fracture size and the consistency of repair kinetics, this method can provide a reasonable means for testing therapeutic targets for fracture healing, osteoporosis, and other tissue regeneration such as skeletal muscle.

Disclosures

The authors declare that they have no competing financial Interests.

Acknowledgements

We thank C. Park for reading the manuscript. This work was supported by the NIAMS under Award Number K01AR061434 and a Leukemia & Lymphoma Society Fellowship Award (5127-09) to D.P and grants of the National Institutes of Health to C.P.L. and D.T.S. The content is solely the responsibility of the authors and does not necessarily represent the official views of the National Institutes of Health.

References

1. Harada, S., & Rodan, G. A. Control of osteoblast function and regulation of bone mass. *Nature*. **423**, 349-355, doi:10.1038/nature01660 nature01660 [pii] (2003).
2. Manolagas, S. C., & Parfitt, A. M. What old means to bone. *Trends Endocrinol Metab*. **21**, 369-374, doi:S1043-2760(10)00024-X [pii] 10.1016/j.tem.2010.01.010 (2010).
3. Khosla, S., & Riggs, B. L. Pathophysiology of age-related bone loss and osteoporosis. *Endocrinol Metab Clin North Am*. **34**, 1015-1030, xi, doi:S0889-8529(05)00090-3 [pii] 10.1016/j.ecl.2005.07.009 (2005).
4. Friedenstein, A. J., Chailakhyan, R. K., Latsinik, N. V., Panasyuk, A. F., & Keiliss-Borok, I. V. Stromal cells responsible for transferring the microenvironment of the hemopoietic tissues. Cloning in vitro and retransplantation in vivo. *Transplantation*. **17**, 331-340 (1974).
5. Mendez-Ferrer, S., *et al.* Mesenchymal and haematopoietic stem cells form a unique bone marrow niche. *Nature*. **466**, 829-834, doi:nature09262 [pii] 10.1038/nature09262 (2010).
6. Park, D., *et al.* Endogenous Bone Marrow MSCs Are Dynamic, Fate-Restricted Participants in Bone Maintenance and Regeneration. *Cell Stem Cell*. **10**, 259-272, doi:S1934-5909(12)00061-6 [pii] 10.1016/j.stem.2012.02.003 (2012).
7. Schindeler, A., McDonald, M. M., Bokko, P., & Little, D. G. Bone remodeling during fracture repair: The cellular picture. *Semin Cell Dev Biol*. **19**, 459-466, doi:S1084-9521(08)00043-8 [pii] 10.1016/j.semcdb.2008.07.004 (2008).
8. Holstein, J. H., *et al.* Rapamycin affects early fracture healing in mice. *Br J Pharmacol*. **154**, 1055-1062, doi:bjp2008167 [pii] 10.1038/bjp.2008.167 (2008).
9. Maes, C., *et al.* Osteoblast precursors, but not mature osteoblasts, move into developing and fractured bones along with invading blood vessels. *Dev Cell*. **19**, 329-344, doi:S1534-5807(10)00338-2 [pii] 10.1016/j.devcel.2010.07.010 (2010).
10. Grcevic, D., *et al.* In vivo fate mapping identifies mesenchymal progenitor cells. *Stem Cells*. **30**, 187-196, doi:10.1002/stem.780 (2012).
11. O'Neill, K. R., *et al.* Micro-computed tomography assessment of the progression of fracture healing in mice. *Bone*. **50**, 1357-1367, doi:10.1016/j.bone.2012.03.008 S8756-3282(12)00726-0 [pii] (2012).
12. Kovar, J. L., *et al.* Near-infrared-labeled tetracycline derivative is an effective marker of bone deposition in mice. *Anal Biochem*. **416**, 167-173, doi:10.1016/j.ab.2011.05.011 S0003-2697(11)00307-1 [pii] (2011).
13. Mayer-Kuckuk, P., & Boskey, A. L. Molecular imaging promotes progress in orthopedic research. *Bone*. **39**, 965-977, doi:S8756-3282(06)00486-8 [pii] 10.1016/j.bone.2006.05.009 (2006).
14. Lo Celso, C., *et al.* Live-animal tracking of individual haematopoietic stem/progenitor cells in their niche. *Nature*. **457**, 92-96, doi:nature07434 [pii] 10.1038/nature07434 (2009).
15. Kuhn, R., Schwenk, F., Aguet, M., & Rajewsky, K. Inducible gene targeting in mice. *Science*. **269**, 1427-1429 (1995).
16. Duran-Struuck, R., & Dysko, R. C. Principles of bone marrow transplantation (BMT): providing optimal veterinary and husbandry care to irradiated mice in BMT studies. *Journal of the American Association for Laboratory Animal Science: JAALAS*. **48**, 11-22 (2009).
17. Tu, Q., *et al.* Osterix overexpression in mesenchymal stem cells stimulates healing of critical-sized defects in murine calvarial bone. *Tissue Eng*. **13**, 2431-2440, doi:10.1089/ten.2006.0406 (2007).

Copyright © 2014 Journal of Visualized Experiments